Interleukin-10 regulates progenitor differentiation and modulates neurogenesis in adult brain

Fernando J. Perez-Asensio[1,2,3], Unai Perpiñá[1,2], Anna M. Planas[1,2] and Esther Pozas[1,2,*]

[1]Unit of Brain Ischemia, Institut d'Investigacions Biomèdiques August Pi i Sunyer, IDIBAPS, 08036 Barcelona, Spain
[2]Department of Brain Ischemia and Neurodegeneration, Institute of Biomedical Research of Barcelona, Consejo Superior de Investigaciones Científicas, CSIC, 08036 Barcelona, Spain
[3]Plataforma de Recerca Aplicada en Animal de Laboratori, Parc Científic de Barcelona, PRAAL-PCB, Baldiri Reixac 10, 08028 Barcelona, Spain
*Author for correspondence (esther.pozas@iibb.csic.es)

Accepted 11 June 2013
Journal of Cell Science 126, 4208–4219

doi: 10.1242/jcs.127803

Summary

The adult subventricular zone (SVZ) is the main neurogenic niche in the adult brain of mice and rats. The adult SVZ contains neural stem cells (NSCs) that primarily differentiate into committed neuroblasts. The newly generated neuroblasts accumulate in dorsal SVZ where they further differentiate and initiate a long migration pathway to their final destination, the olfactory bulb (OB). Here, we report a new role for Interleukin 10 (IL-10) that is different to its well-known anti-inflammatory properties. We show that the IL-10 receptor is expressed in Nestin-positive progenitors restricted to the dorsal SVZ in adult brain. Using IL-10 gain models, we observed that IL-10 maintains neural progenitors in an undifferentiated state by keeping progenitors in an active cycle where pro-neural gene markers (Nestin, Sox1, Sox2, Musashi, Mash1) are upregulated and neuronal gene expression (Numb, DCX, TUBB3) is downregulated. In addition, IL-10 reduces neuronal differentiation and ultimately impairs endogenous neurogenesis. Consistently, in the absence of IL-10, *in vivo* neuronal differentiation of SVZ progenitors is enhanced and the incorporation of new neurons in the adult OB is increased. Thus, our results provide the first evidence that IL-10 acts as a growth factor on SVZ progenitors and regulates neurogenesis in normal adult brain.

Key words: Adult neurogenesis, Cytokines, Neural stem cell, Neuronal differentiation

Introduction

The subventricular zone (SVZ) of the lateral ventricle (LV) is the main neurogenic area in the adult murine brain. The neural stem cells (NSCs, Type B cells) present in the SVZ are astrocytes characterized by long cell cycles and GFAP expression. NSCs give rise to rapid transit amplifying dividing cells (TAPs) or Type C cells ($GFAP^-$, $EGFR^+$, $Ki67^+$ and $Mash1^+$). Most cells that arise in the SVZ generate neuroblasts (Type A cells: PSA^-, $NCAM^+$, DCX^+, $TUBB3^+$), which migrate over long distances through a rostral migratory pathway (RMS) to reach the olfactory bulb where they finally become mainly GABAergic interneurons (Doetsch and Alvarez-Buylla, 1996; Doetsch et al., 1997; Lois and Alvarez-Buylla, 1994; Merkle et al., 2004). Also, under physiological conditions, oligodendrocytes ($Olig2^+$, $Ng2^+$) and a small number of glutamatergic neurons ($Tbr2^+$, $vGlut2^+$) are generated in the SVZ (Brill et al., 2009; Gonzalez-Perez et al., 2009; Marshall et al., 2005; Menn et al., 2006; Parras et al., 2004). Nestin is a cell marker for NSCs, but it remains expressed in TAPs ($Mash1^+$) and immature committed neuroblasts ($TUBB3^+$) (Doetsch et al., 1997). The adult SVZ is an extensive area where proliferation and neurogenesis occur along the entire rostrocaudal and dorsoventral axes (Mirzadeh et al., 2008). Experiments with viral or genetic lineage tracing indicate that the SVZ is arranged as a mosaic. The position of NSCs within the SVZ determines the types of differentiated progeny generated. In particular, deep granule interneurons and a subpopulation of periglomerular cells arise from the ventral SVZ, whereas superficial granule interneurons, distinct periglomerular cells, and glutamatergic cells are derived from the dorsal SVZ (Brill et al., 2009; Ihrie et al., 2011; Kohwi et al., 2007; Young et al., 2007; Merkle et al., 2007). Progenitors generated along the entire ventral and dorsal regions of the SVZ move from the walls of the LV by means of a series of complex migratory movements to reach more anterior dorsal SVZ regions and form complex interconnected chains to incorporate into the RMS and reach the OB (Kakita and Goldman, 1999; Geraerts et al., 2006; Sawamoto et al., 2006; Nam et al., 2007). Postnatal neurogenesis is regulated by physiological and pathological conditions, and the integration of extracellular signaling activation and the presence of some intrinsic mechanisms lead to cell fate determination and lineage differentiation (Guillemot, 2007; Lim et al., 2009). The identity and lineage of stem cells has been elucidated; however, the regulatory mechanism underlying stem cell renewal, survival and differentiation *in vivo* are not fully understood (Aguirre et al., 2010; Androutsellis-Theotokis et al., 2006; Andreu-Agulló et al., 2009; Ramírez-Castillejo et al., 2006; Fernando et al., 2011; Khodosevich et al., 2010; Mobley et al., 2009; Rabaneda et al., 2008; Romero-Grimaldi et al., 2012; Teixeira et al., 2012). NSC self-renewal is modulated by several factors, such as VEGF and PEDF, which are released by ependymal and endothelial cells, and the Notch mechanism plays a crucial regulatory function in this process (Aguirre et al., 2010; Andreu-Agullo et al., 2009; Androutsellis-Theotokis et al., 2006; Marqués-Torrejón et al., 2013; Ramírez-Castillejo et al., 2006). Although these events

have been extensively studied in the ventral part of the LV, the regulatory mechanisms acting on progenitor cell proliferation and differentiation in the dorsal SVZ before these cells enter the RMS to regenerate the OB are unclear.

IL-10 is a general anti-inflammatory molecule that is present at low levels in circulating blood. It exerts key functions for the maintenance of the pro- and anti-inflammatory balance in the body to prevent inflammatory and autoimmune pathologies (Ouyang et al., 2011; Pestka et al., 2004; Saraiva and O'Garra, 2010). Here we demonstrate a new physiological role for this cytokine. We found that IL-10 activity targeted the whole heterogeneous population of Nestin$^+$ progenitors, generated along the entire SVZ, when these cells were present in the dorsal SVZ region to later enter the RMS. When Nestin$^+$ progenitors were present in dorsal SVZ, IL-10 upregulated the expression of undifferentiated neural progenitor cell markers, the number of progenitors in the active cell cycle and the inhibitory phosphorylation of CDC2. Subsequently, neuronal differentiation was impaired and the number of postmitotic neuroblasts reduced.

Results

Components of IL-10 signaling are regionally present in the adult SVZ

IL-10 signals through two membrane receptor chains, IL-10R1 and IL-10R2 (Pestka et al., 2004). IL-10R2 is widely expressed in the brain. By contrast, IL-10R1 expression is low in normal brain, and the activation of this subunit is responsible for STAT3 docking, which mediates intracellular signaling (Pestka et al., 2004; Gonzalez et al., 2009). Here we focused on the expression of IL-10 and its receptor in the SVZ in rat and mouse brain. A similar expression pattern was detected in both species. Regular RT-PCR showed the presence of IL-10R1 transcripts in postnatal (P) and adult (Ad) SVZ tissue, as well as in primary cultures of postnatal SVZ (supplementary material Fig. S1). IL-10 mRNA was expressed in cell cultures, and low levels of this molecule were detected in brain samples (supplementary material Fig. S1). In order to determine the spatial distribution of IL-10R1 in the whole SVZ, we performed histological studies on a series of rostrocaudal coronal sections from adult brain. IL-10R1 expression was detected from dorsal to ventral sub-regions of the SVZ (Fig. 1A) and in migrating cells (Nestin$^+$) in the RMS (Fig. 1B), whereas no staining was detected in the OB (data not shown). A representative drawing of a coronal section in Fig. 1 indicates the ventral and dorsal regions analyzed. Confocal imaging showed that, in the entire SVZ, IL-10R1 is expressed in the cell monolayer that limits the LV, where ependymal cells are located (Fig. 1A, arrows). Double-immunofluorescence analysis corroborated the presence of IL-10R1 in cells positive for S100B, a marker for ependymal cells in dorsal and ventral SVZ regions (Fig. 1C,D). In ventral areas, Nestin$^+$ progenitors grouped in patches in a second line of cells next to the open ventricle and did not express IL-10R1 (Fig. 1C, arrow). By contrast, in the dorsal region of the SVZ, IL-10R1 staining was observed in a wide lateral zone next to the open ventricle, and this staining matched the region where Nestin$^+$ progenitors were located (Fig. 1D). High-magnification confocal pictures demonstrated the presence of IL-10R1 on the cellular limits of Nestin$^+$ cells (Fig. 1D, arrowheads, bottom panels).

Double-labeling confocal images were analyzed on coronal sections containing the subgranular zone (SGZ) of the hippocampus, the second neurogenic niche of the adult brain.

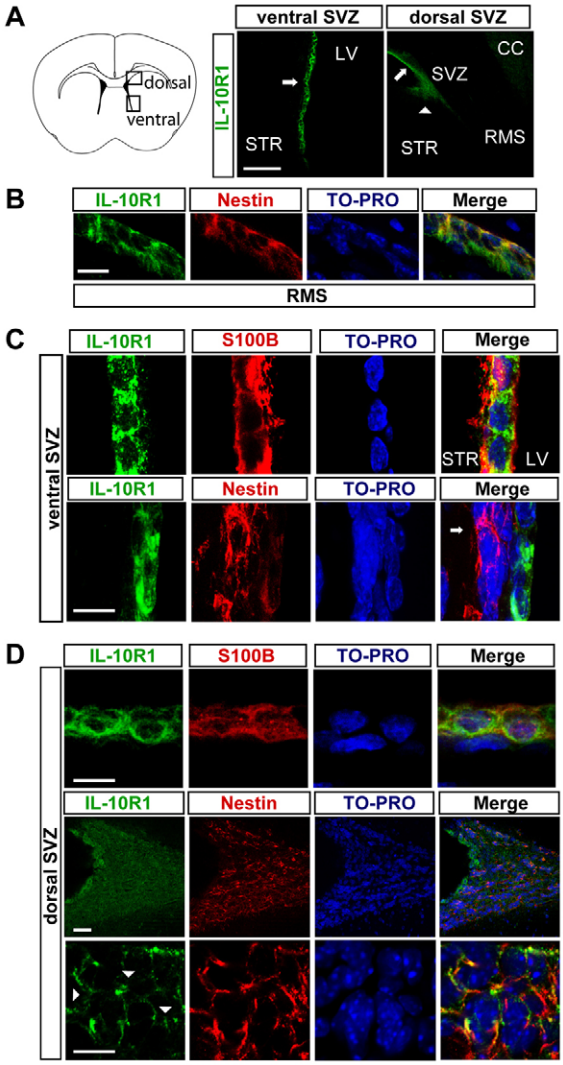

Fig. 1. Expression of IL-10 receptor in adult SVZ. (A) Expression of IL-10R1 in the entire SVZ on adult rat brain sections. IL-10R1 localizes to both ventral and dorsal sub-regions into cells lining the adult lateral ventricle. In dorsal SVZ the IL-10R1 staining was more extensive adjacent to the open ventricle (arrow). (B) IL-10R1 (green) signal was present in Nestin$^+$ (red) progenitors along the RMS. (C) Expression of IL-10R1 in ventral SVZ sub-region of adult rat brain sections. Double immunofluorescence demonstrates that strong S100$^+$ (red), a marker of ependymal cells, colocalizes with IL-10R1 (green). By contrast, Nestin$^+$ progenitors (red) are IL-10R1 negative in ventral SVZ (arrow). (D) Expression of IL-10R1 on dorsal SVZ on adult rat brain sections. Dorsal S100$^+$ cells (red) also express IL-10R1 (green). A vast dorsal region where Nestin$^+$ (red) progenitors are located is also positive for IL-10R1 staining. High-resolution images show how IL-10R1 staining is present in the cellular limits of Nestin$^+$ (red) progenitors (arrowhead). TO-PRO (blue) stains all nuclei. CC, cerebral cortex; LV, lateral ventricle; RMS, rostral migratory stream; STR, striatum; SVZ, subventricular zone. Scale bars: 100 μm (A); 50 μm (B); 20 μm (C,D).

Staining revealed that Nestin$^+$ (red) cells and DCX$^+$ neuroblasts (red) do not express IL10-R1 (green) (supplementary material Fig. S2), thereby suggesting that IL-10 does not act on the adult hippocampal neurogenic niche.

To identify the SVZ cell phenotype expressing IL-10R1, we analyzed the expression of this protein in dissociated cultures of

dorsal regions of the whole SVZ at high confocal resolution. IL-10R1 colocalized with the membrane-associated protein Spectrin, thereby indicating that the IL-10 receptor is present in cellular membranes, as expected for an active receptor (Fig. 2A). Immunofluorescence analysis also demonstrated the presence of IL-10R1 (green) in most of the cultured cells (79.5±4.3%). Double-immunofluorescence analysis with cellular markers revealed that nearly all Nestin$^+$ progenitors were IL10R1$^+$ (96.89±1.6%; $P<0.01$; Fig. 2A,B) and most TUBB3$^+$ committed neuroblasts (red) expressed IL-10R1 (79.3±% 5.0; $P<0.01$; Fig. 2A,B).

The unexpected IL-10R1 expression pattern described here points to a new unknown biological activity for IL-10 in the adult SVZ neurogenic niche. Nestin is a marker of NSCs but its expression remains in intermediate progenitors, including a subpopulation of immature neuroblasts (Doetsch et al., 1997). Nearly all Nestin$^+$ progenitors obtained from the whole dorsal SVZ expressed Il-10R1; this observation is compatible with IL-10 signaling in a majority and heterogeneous population of progenitors at different steps of differentiation. This suggests that when these cells are located dorsally and entering the RMS, IL10 signaling is involved in the modulation of adult progenitor neurogenesis.

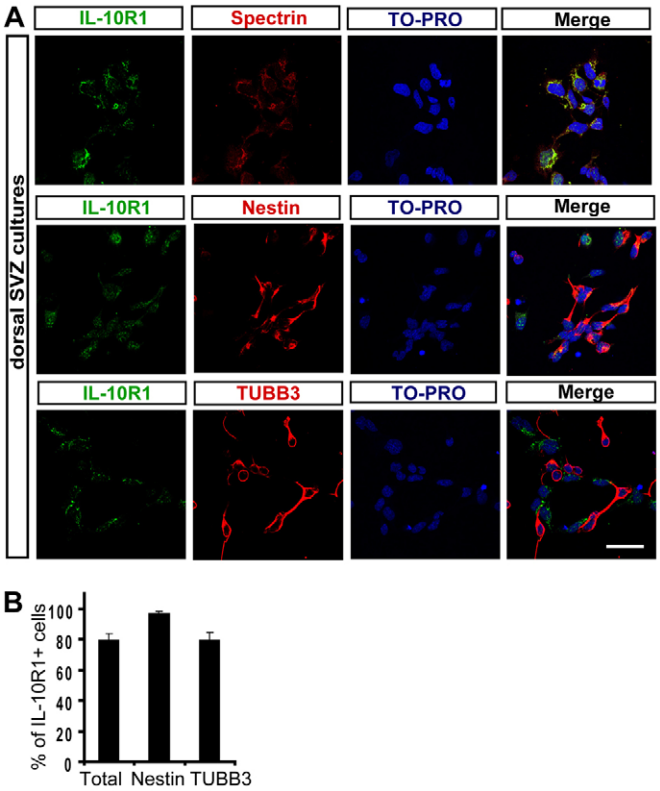

Fig. 2. Nestin$^+$ progenitors and neuroblasts express IL-10R1. (A) Immunofluorescence of IL-10-R1 (green), Spectrin (red), Nestin (red) and TUBB3 (red) on dissociated primary cultures of SVZ from rat brain. Staining of isolated cells reveals that IL10-R1 colocalizes with Spectrin, a membrane-associated protein. Double staining with cell type markers confirmed that the vast majority of Nestin$^+$ progenitors and TUBB3$^+$ neuroblasts expressed IL-10R1. (B) Histograms summarized as a percentage of IL-10R1-positive cells (means ± s.e.m.) in total or specific subset populations. TO-PRO stained all nuclei (blue). Scale bar: 25 μm.

IL-10 does not alter self-renewal of SVZ neural stem cell cultures

To explore the effects of IL-10 on NSCs, we performed neurosphere assays and assessed the effects of this molecule on the stem cell population (Ferron et al., 2007). It should be taken into account that a number of TAPs also develop as neurospheres in this culture model (Pastrana et al., 2011).

The number of secondary neurospheres increased in the presence of IL-10 (Fig. 3A). To evaluate whether IL-10 improved cell survival, secondary neurospheres were triturated, and cell viability was evaluated by the Trypan Blue exclusion assay. No differences were observed between treated and untreated neurospheres, thus showing that cell survival was not

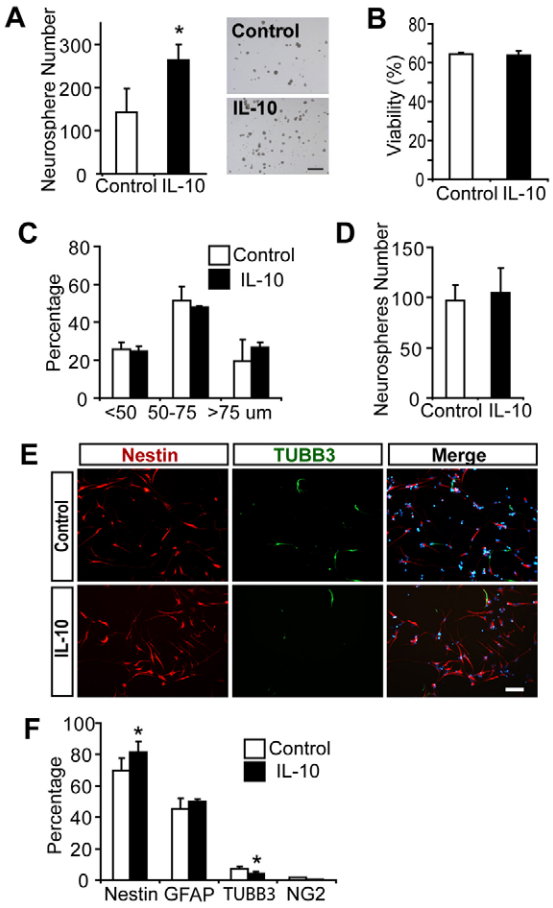

Fig. 3. IL-10 regulates differentiation but does not alter self-renewal of NSCs from SVZ. (A) The number of secondary neurospheres increases after addition of IL-10. (B) Cell viability (Trypan Blue exclusion) was similar between control and IL-10-treated cultures ($n=3$). (C) Neurosphere-size distribution was unchanged by IL-10 ($n=6$). (D) Generation of tertiary neurospheres in the absence of IL-10 was similar between previously IL-10-treated and untreated secondary neurospheres ($n=4$). (E) Presence of neural cells after 7-day neurosphere differentiation. Images illustrating the impaired neurogenesis after IL-10 treatment. A higher number of Nestin$^+$ (red) cells and reduced number of neuroblasts (green) were detected. Hoechst 33342 (blue) stained all nuclei ($n=5$). (F) Histogram represents how addition of IL-10 elevates the number of original Nestin$^+$ cells and specifically induces a decrease in the number of neuroblasts (TUBB3$^+$ cells) without affecting oligodendroglial differentiation (NG2$^+$ cells) ($n=5$). Scale bars: 100 μm (A); 40 μm (E). Data are means ± s.e.m.; *$P<0.05$.

enhanced by this cytokine (Fig. 3B). Furthermore, analysis of neurosphere sizes manifested a normal distribution in treated and untreated cultures, indicating that IL-10 had no effect on proliferation rates (Fig. 3C) (Ferron et al., 2007). To decipher the impact of IL-10 on self-renewal, secondary neurospheres, either exposed or non-exposed to this cytokine, were passaged in the absence of IL-10. The number and size distribution of newly formed tertiary neurospheres were similar between previously IL-10-treated or untreated secondary neurospheres (Fig. 3D), indicating that this cytokine did not affect NSC self-renewal. Consequently, the higher number of secondary neurospheres observed in the presence of IL-10 could be explained by a direct growth effect induced by this molecule on NSCs or TAPs and suggests that IL-10 acts as a factor promoting maintenance of neural progenitors in an undifferentiated state. When tertiary neurospheres were disaggregated and cultured in differentiating conditions, the presence of IL-10 maintained a higher population of NSCs in culture ($Nestin^+$ cells, undifferentiated) and neurogenesis was reduced ($TUBB3^+$ cells), whereas glial differentiation was maintained (Fig. 3E,F).

The neurosphere assay was performed in both rat and mouse samples, and comparable outcomes were observed in both species. Together, these results suggest that IL-10 acts on neural SVZ progenitors and plays a role in the regulation of neuronal differentiation.

IL-10 activity increases the presence of undifferentiated progenitors and delays cell cycle exit, thereby causing a reduction in neuronal differentiation in SVZ-dissociated cultures

To evaluate the direct effect of IL-10 on SVZ progenitors, we used a more direct culture than the neurosphere assay to better represent the heterogeneous population present in the whole dorsal SVZ *in situ*. For this purpose, we performed monolayer primary cultures from dissociated cells from whole dorsal postnatal SVZ from rats; unfortunately, mouse cultures did not attach properly in these conditions. Cells were cultured in medium conditions similar to those used for the neurosphere differentiation assay with the absence of mitogenic factors. Microglial ($IBA1^+$) cells were not detected in monolayer culture conditions. These cultures consisted of a heterogeneous cell population in which proliferation and differentiation occurred (Fig. 4A,D). As observed in the neurosphere culture, IL-10 did not affect cell viability or proliferation (PI and BrdU incorporation, respectively); however, the number of cells in active cell cycle ($Ki67^+$) increased (Fig. 4A), thus pointing to an effect of this cytokine on cell cycle activity. Moreover, IL-10 upregulated neural markers such as Nestin, Sox1, Sox2, Musashi and Mash1, as well as activated Notch (NICD) (Fig. 4B), thereby suggesting that this cytokine causes a more pronounced undifferentiated progenitor state in SVZ cells. By contrast, the expression of Numb, a protein involved in neuronal differentiation (Imai et al., 2001; Kuo et al., 2006; Li et al., 2003; Nishimoto et al., 2010; Petersen et al., 2004) was reduced (Fig. 4B). Actin was unaltered and used as a loading control (Fig. 4B). Phenotypic analysis of monolayer cultures by immunofluorescence showed that, in the presence of IL-10, undifferentiated neural cell types accumulated, whereas the number of cells with a neuronal phenotype decreased. The number of $Nestin^+$ cells markedly increased, and these cells underwent considerable morphological changes (Fig. 4C,D). They had more pronounced long processes that resembled the radial processes of radial glia, its developmentally originary cell (Fig. 4C, arrow; Merkle et al., 2004). Moreover, IL-10 increased the number of cells positive for Mash1, which is a marker for the TAP population (42.4±4.7%, Fig. 4D). By contrast, this cytokine decreased the number of neuroblasts ($TUBB3^+$ cells; 53.03±3.8% in controls versus 33.7±1.7% in IL-10-treated animals) and induced a higher proportion of $TUBB3^+$ cells that co-expressed Nestin (66.6±1.7% in controls versus 81.1±1.9% in treated cells) and were in the active cell cycle (11.3±1.5% in controls versus 18.4±0.9% in IL-10-treated animals). The numbers of glial progenitors (either $Olig2^+$ or $NG2^+$ cells) were unchanged after IL-10 treatment (Fig. 4D; and data not shown). Together, our results indicate that IL-10 does not interfere with the cell proliferation rate but does induce the accumulation of undifferentiated progenitors, which reduces neurogenesis. This finding suggests that IL-10 participates in the G2–M cell cycle transition.

To decipher alterations in this transition, we analyzed the presence of mitotic cells by staining for the phosphorylated form of histone 3 (PH3) as an M-phase-specific marker. The percentage of $PH3^+$ cells was reduced by the presence of IL-10 at a range of post-treatment times (Fig. 4E, increase versus initial time). Furthermore, to determine whether IL-10 slowed down cell cycle progression through G2–M, a series of BrdU pulses (time 0), followed by various chase times, were conducted. Between 8 and 10 hours of chase, $BrdU^+$ cells duplicated, indicating that this is the period required to transit to G2–M in order to leave the cell cycle (data not shown). To assess the acute effects of IL-10 on the S to M transition, BrdU labeling was combined with staining for PH3. At 3 and 6 hours, IL-10-treated cultures showed a lower percentage of double-labeled cells ($BrdU^+$, $Ph3^+$) (Fig. 4F). Moreover, at 6 hours, a higher number of cells left the cell cycle ($BrdU^+$, $Ki67^-$) in the control cultures (Fig. 4G,H). These findings support the notion that IL-10 delays the G2–M transition and subsequently the exit of the SVZ dorsal progenitors from the active cell cycle.

The continuation of mitosis universally involves early activation of M-phase-promoting factor by dephosphorylation of the inhibitory Thr14- and Thr15-phosphorylated sites of CDC2 protein kinase (Abrieu et al., 1997). We analyzed whether this key mechanism that controls G2–M cell cycle progression is regulated by IL-10. This cytokine induced a robust increase in CDC2 phosphorylation without affecting the total levels of expression of this cell cycle regulator in cultures (Fig. 4I). The increase in pCDC2 was due to an increase in the number of $pCDC2_{Tyr15+}$ cells, which were mainly $Nestin^+$ (Fig. 4J). Moreover, IL-10 increased the percentage of $TUBB3^+$ neuroblasts showing $pCDC2_{Tyr15}$ (13.7±0.2 in controls versus 21.2±0.3% in IL-10-treated animals, Fig. 4K). These findings suggest that IL-10 directly promotes a neural profile of SVZ cells while also impairing cell cycle exit and accumulating progenitors in G2–M transition, thus preventing these cells from dropping out of the cell cycle to become fully differentiated neurons.

The effects of IL-10 were also assayed in SVZ explants. Postnatal SVZ explants contained a population of $Nestin^+$ cells restricted to zones near the core of the explants, whereas TUBB3 and DCX neuronal markers were present in migrating precursors, which also expressed IL-10R1 (Fig. 5A). When SVZ dorsal explants were exposed to IL-10, the area of migrating cells moving away from the core of the explants was severely reduced

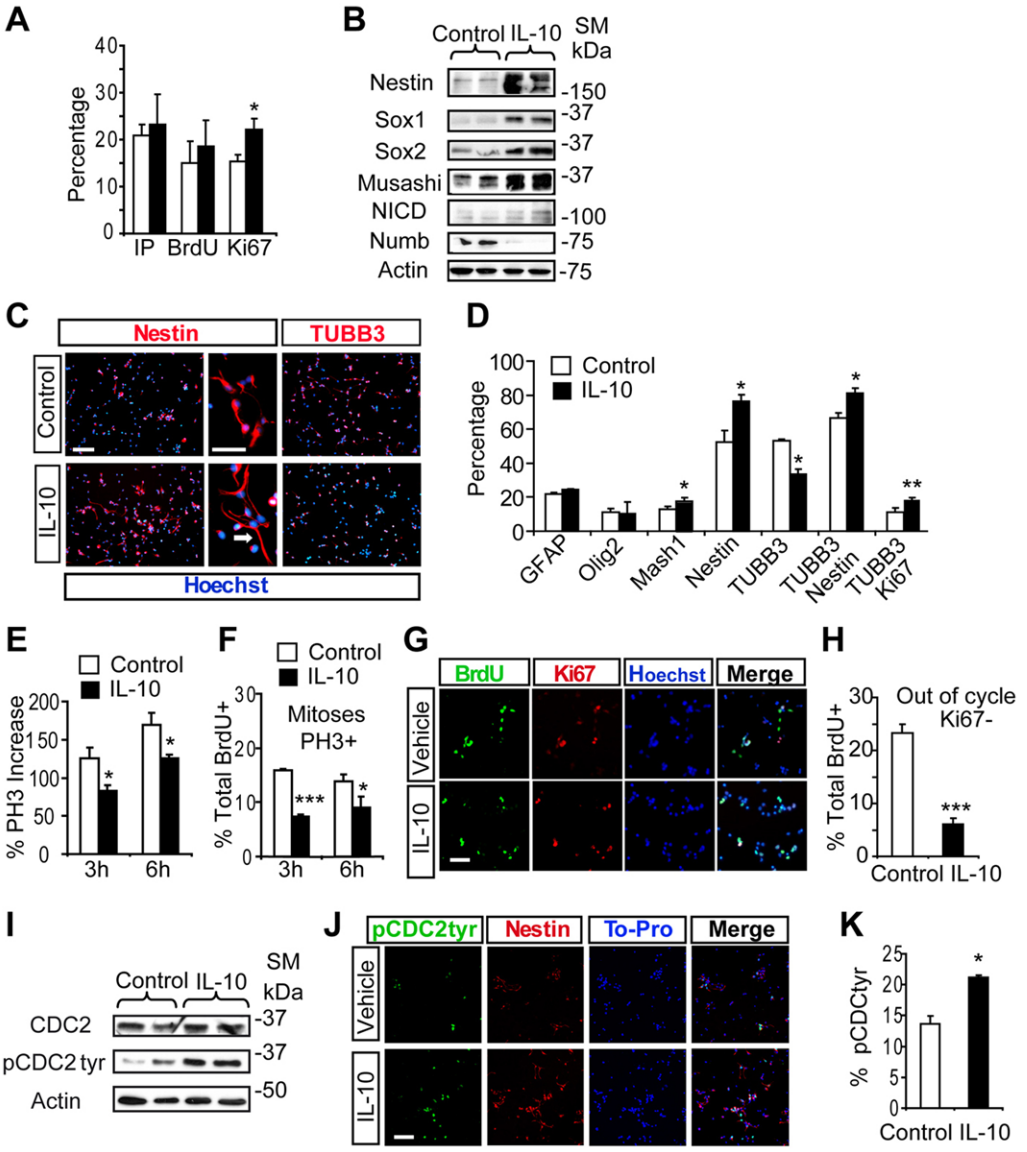

Fig. 4. IL-10 alters cell cycle exit and upregulates the expression of genes related to undifferentiated state in SVZ neural progenitors. (A) Histograms represent percentage cell viability (IP), proliferation (BrdU) and number of cell in active cycle (Ki67) in the presence or absence of IL-10 (50 ng/ml) in differentiating primary cultures from rat brain. IL-10 does not alter cell survival or proliferation, but increases the number of Ki67^{+} cells (n=6). (B) Protein expression of neural and general markers after 48 hours of IL-10 treatment in primary cultures (50 ng/ml). In neural progenitors cultures, the expression of undifferentiated markers such as Nestin, Sox1 and Sox2, Musashi and NICD were robustly induced in the presence of IL-10; Numb was severely reduced; actin was used as a loading control (n=5). (C) Immunofluorescence images of primary SVZ cultures illustrating the increase of Nestin^{+} progenitors (red) and the reduction of neuroblasts (TUBB3^{+}, red) after IL-10 treatment for 4 days (n=5). In high-resolution images arrows indicate the long process develop by Nestin^{+} cells in the presence of IL-10. Hoechst 33342 (blue) stained all nuclei. (D) Graph summarizes the presence of cellular markers after IL-10 treatment. The number of Ki67^{+}, Nestin^{+} and Mash1^{+} cells increased, and TUBB3^{+} cells decreased in the presence of IL-10 (as a percentage of total cells). In the pool of TUBB3^{+} cells, a higher proportion of cells expressed Nestin and were active in the cell cycle (Ki67^{+}). Glial markers such as GFAP and Olig2 were unchanged (n=5). (E) Graph illustrates a reduced proportion of cells that reach mitosis (PH3^{+}) in IL-10-treated cultures. Differences are represented as a percentage versus the initial time (time 0) (n=4). (F) IL-10 cultures had a consistent decrease in the number of BrdU^{+} and PH3^{+} cells in the 3-hour and 6-hour groups (n=4). (G) Immunofluorescence for BrdU (green) and KI67 (red) in SVZ cultures at 6 hours (n=4).TO-PRO (blue) stained all nuclei. (H) The percentage of BrdU^{+} cells that drop out of the cell cycle (KI67^{-}) was dramatically reduced in the presence of IL-10 at 6-hour chased group (n=4). (I) Total amount of the cell cycle regulator CDC2 was unchanged after IL-10 treatment. The amount of phosphorylated pCDC2$_{Tyr15}$ increased after treatment. Actin was used as a loading control (n=4). (J) Immunofluorescence for pCDC2$_{Tyr15}$ (green) in SVZ cultures shows the presence of the phosphorylated protein in Nestin^{+} (red) cells (n=4). TO-PRO (blue) stained all nuclei. (K) IL-10 increases the percentage of neuroblasts that are positive for pCDC2$_{Tyr15}$. SM: standard molecular size marker. Scale bars: 30 μm (C,G,J). Data are means ± s.e.m.; *P<0.05, **P≤0.01, ***P≤0.001.

(Fig. 5B). Furthermore, analysis of explants of dorsal SVZ from IL-10-deficient mice (IL-10-KO) (Kühn et al., 1993) revealed that in the endogenous absence of this cytokine, the area of migrating cells was significantly increased when compared with WT explants (Fig. 5C). These observations could be explained by an impairment of neuronal differentiation;

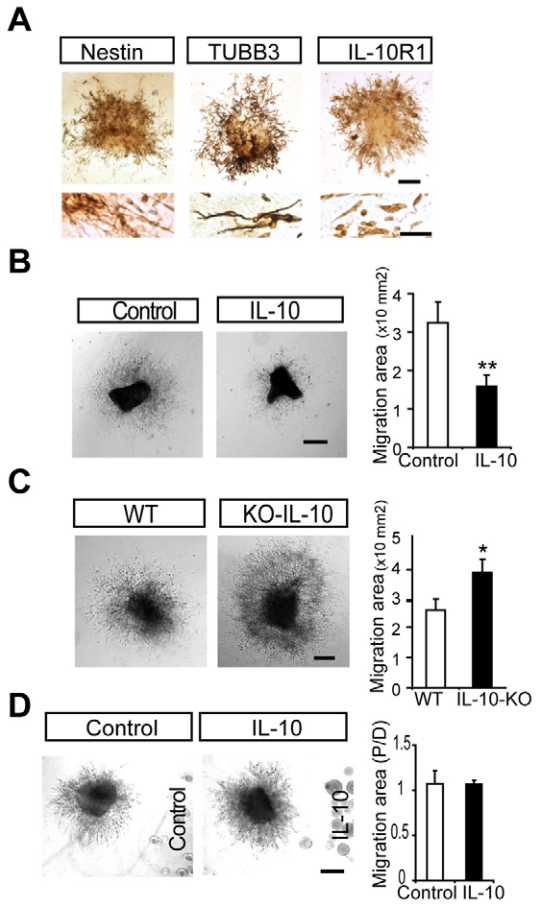

Fig. 5. IL-10 levels alter cell exit from SVZ explants but do not exert any chemoeffect. (A) Immunohistochemistry of neural proteins on SVZ postnatal explants. Nestin is localized in cells located near the core of explants and TUBB3 is found in migrating cells. IL10-R1 is expressed in some cells exiting the explants. (B) Bright-field images showing that IL-10 reduces the migration area of progenitors exiting postnatal explants of the SVZ (n=4). (C) Bright-field images showing the migration area detected on postnatal SVZ explants from IL-10-KO animals is higher compared with WT explants (n=3). (D) Bright-field images showing progenitor migration on postnatal SVZ explants confronted with a source of IL-10. The ratio of migration area of proximal (P) versus distal (D) region of the explants was similar between explants exposed to a source of BSA or IL-10 (n=3). Scale bars: 100 µm. Data are means ± s.e.m.; *P≤0.05, ***P≤0.01.

however, IL-10-mediated effects on cell migration cannot be excluded. To rule out this possibility, we performed a migration assay where SVZ explants were confronted by a source of IL-10 (IL-10 soaked beads). No chemorepulsive or chemoattractive effects were induced by IL-10 on SVZ progenitors (Fig. 5D).

All together, these results indicate that the action of IL-10 on SVZ Nestin$^+$ progenitors regulates neurogenesis by causing a delay in the G2–M cell cycle progression and promoting an undifferentiated neural stage in dorsal SVZ progenitors.

IL-10 increases the population of progenitors in detriment to committed neuroblasts *in vivo*

We developed an *in vivo* gain-of-function model to decipher the physiological role of IL-10. The LV (right hemisphere) of adult mouse brains was infused with this cytokine at very low doses over 7 days (IL-10-gain). BrdU was administered to the animals once daily to monitor newly born cells. Histological studies were carried out in the left hemisphere, contralateral to that receiving the cannula implantation. The expression levels of astroglial (supplementary material Fig. S3A) and microglial (supplementary material Fig. S3B) markers such as GFAP and Iba-1 were similar between control and IL-10-gain animals, showing that IL-10 did not induce a glial reaction, as an indication that neuroinflammation was not altered.

Histological exploration of the ventral SVZ sub-region showed that both proliferating (PCNA$^+$ cells, 339±40.2 versus 292±14.2) and cycling (Ki67$^+$, 189±32.3 versus 217±50.6) cells were observed in the ventral neurogenic niche and indicated that IL-10 did not affect these specific progenitors, as expected because Nestin$^+$ ventral progenitors are negative for IL-10-R1.

In-depth histological analyses of the dorsal SVZ indicated no changes in the total number of exiting cells (TO-PRO$^+$) or cell death (see Materials and Methods) in the IL-10-gain *in vivo* model. Likewise, the numbers of newly generated (BrdU$^+$) and PCNA$^+$ cells (164±17.8 versus 160±5.4) were similar between control and IL-10-treated animals, thus supporting the notion that proliferation was not altered (Fig. 6A,B). However, the number of cells in the active cycle (Ki67$^+$ cells) increased (Fig. 6A,B). Moreover, the expression of neural undifferentiating markers, such as Nestin, Musashi, NICD and Mash1, were increased in the IL-10 gain-of-function model (Fig. 6C). By contrast, NUMB and the neuronal marker DCX were severely reduced (Fig. 6C). The loading control, actin, was unaltered (Fig. 6C). Studies on sections at the cellular level revealed a sharp increase in the number of Nestin$^+$ and Mash1$^+$ cells in the dorsal SVZ after IL-10 treatment (Fig. 6D,E). By contrast, the number of committed neuroblasts (either DCX$^+$ or PSA-NCAM$^+$ cells) was significantly reduced (Fig. 6D,E). The percentage of newly generated progenitors (Nestin$^+$, BrdU$^+$) and neuroblasts (DCX$^+$, BrdU$^+$) decreased (Fig. 6F); however, a higher proportion of neuroblasts were actively cycling (DCX$^+$, Ki67$^+$, Fig. 6F). These observations showed that IL-10 does not affect the number of newly born cells. IL-10 intervenes in the existing pool of Nestin$^+$ progenitors located dorsally, in which it promotes the prevalence of an undifferentiated transition state that leads to the impairment of neuronal differentiation. In this regard, the numbers of Nestin$^+$ progenitors and DCX$^+$ neuroblasts recovered in the dorsal SVZ of IL-10-gain animals two weeks after cytokine treatment was stopped (supplementary material Fig. S4A,B).

To further support the relevance of IL-10 as a regulator of the adult SVZ niche, we analyzed endogenous neurogenesis in IL-10-KO mice. Expression analysis of brain samples from these animals showed a reduction in the expression of Nestin and neural markers Musashi and NICD, in the dorsal SVZ (Fig. 6G,H). By contrast, DCX expression was strongly increased (Fig. 6G,H).

In addition, we evaluated NSC self-renewal *in vivo* in these models by assessing the presence of long cells retaining BrdU (LCR) (Ferron et al., 2007). Alteration of IL-10 expression either by gain-of-function or knockout did not induce differences in the number of LCR$^+$ cells in the adult SVZ (supplementary material Fig. S5A,B). This finding indicates that IL-10 does not influence self-renewal *in vivo* and that its effects are related to its contribution to the maintenance of an undifferentiated pool of progenitors.

IL-10 regulates neuronal differentiation in the SVZ niche, causing a final modulation of neurogenesis in the OB

To precisely define whether IL-10 affects the phenotypic diversity of original progenitors *in vivo*, we administered a

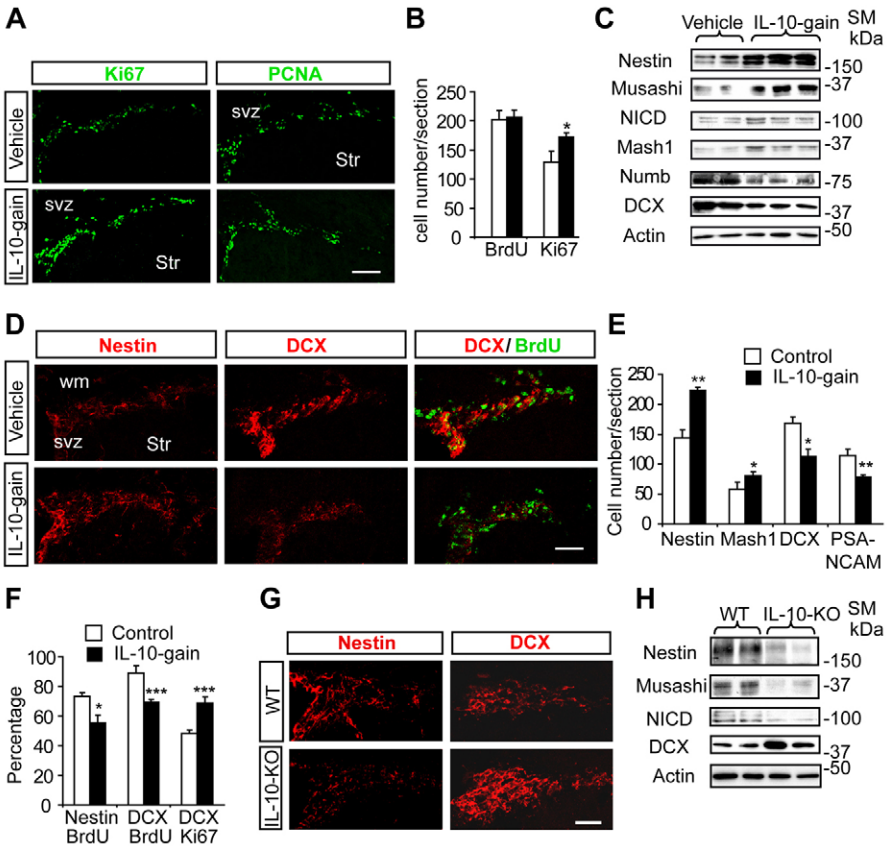

Fig. 6. IL-10 modulates the transition from undifferentiated neural progenitor to neuronal differentiation *in vivo*. (A) The increase of Ki67 and the permanence of PCNA cells in dorsal SVZ after *in vivo* gain-of-function of IL-10 (n=4). (B) Histogram represents the total number of positive cells in the dorsal SVZ. BrdU$^+$ cells are unchanged and Ki67$^+$ cells are increased in IL-10 gain-of-function animals. (C) *In vivo* IL-10 infusion induces the presence of undifferentiated neural progenitor gene markers such as Nestin, Musashi, Mash1 and NICD on dorsal SVZ. Levels of Numb and the neuronal marker DCX were decreased. The level of actin, which served as a loading control, was unchanged (n=6). (D) Dorsal SVZ showing increase of Nestin$^+$, decrease in DCX$^+$ and no differences in BrdU$^+$ cells of IL-10 gain-of-function animals. (E) Quantification summarizes the enlargement in Nestin$^+$ progenitor cells and Mash1$^+$ intermediate progenitor population and the decrease in neuroblasts (DCX$^+$ or PSA-NCAM$^+$) in the SVZ niche of IL-10-treated animals (n=6). (F) Graph shows how IL-10 reduces the percentage of newly generated (Nestin$^+$, BrdU$^+$) neural progenitors and neuroblasts (DCX$^+$, BrdU$^+$) (n=6). Moreover, a higher percentage of neuroblasts are cycling (DCX$^+$, Ki67$^+$). (G) Pictures of dorsal SVZ sections illustrate the decrease in Nestin and the increase in DCX expression in IL-10-deficient cells. (H) In the absence of IL-10, the expression of markers of neural progenitor cells such as Nestin, Musashi and NICD was notably reduced, whereas expression of the neuronal marker DCX increased. Actin was used as a loading control (n=6). Scale bars: 50 µm. Data are means ± s.e.m. *P<0.05, **P≤0.01, ***P<0.001.

single injection of BrdU followed by 4 days of IL-10 treatment. Four days is the required time to detect newly formed neuroblasts in SVZ regeneration experiments (Doetsch et al., 1999). This approach allowed us to confirm that under physiological conditions the SVZ is mainly a neurogenic region because 64.1±2.3% of newly generated cells became committed neuroblasts (BrdU$^+$, DCX$^+$) whereas only 6±3.3% of BrdU$^+$ cells expressed Olig2 as a marker of glial progenitors (Fig. 7A). The number of BrdU$^+$ cells was similar in IL-10 gain animals and the control group, but IL-10 selectively reduced the proportion of committed neuronal cells to 50±2.6%, whereas it did not affect the number of BrdU and Olig2 double-labeled cells (4.5±1.3%) (Fig. 7A). In conclusion, IL-10 reduced neurogenesis by decreasing the pool of committed neuronal progenitors without inducing a switch to a glial phenotype. To further support the relevance IL-10 as a regulator of adult neurogenesis, we analyzed endogenous neurogenesis in IL-10-KO mice. In IL-10-deficient animals the number of new neurons (BrdU$^+$, DCX$^+$) was enhanced (84.9±1.4% versus 70.5±4.1% of WT) after four days of BrdU administration (Fig. 7B). No differences in the number of newly generated glial cells were observed between the two genotypes (BrdU$^+$, Olig2$^+$, 6.9±1.1% versus 6.1±0.6%) (Fig. 7B).

Finally, to study whether the effects of IL-10 on the SVZ influences final neurogenesis, we analyzed the OB (the final target area of newly generated neurons) of IL-10 gain- and loss-of-function animal models. The experimental design consisted of BrdU administration at days 0 and 1 followed by 19 monitoring days. This waiting time is required to allow newly formed cells to become fully differentiated neurons (NeuN$^+$) and reach the OB, the target area (Doetsch and Alvarez-Buylla, 1996). Immunoanalysis of the OB of the IL-10 gain animals showed a reduced number of BrdU$^+$ cells and also a decrease in the total number of newly generated neurons (Brdu and NeuN double-positive cells) (Fig. 7C,D). By contrast, IL-10 deficiency caused a significant increase in the number of newly formed cells (BrdU$^+$) and neurons (BrdU$^+$, NeuN$^+$) that incorporated into the OB (Fig. 7E,F). Moreover, western blot analysis of OB samples

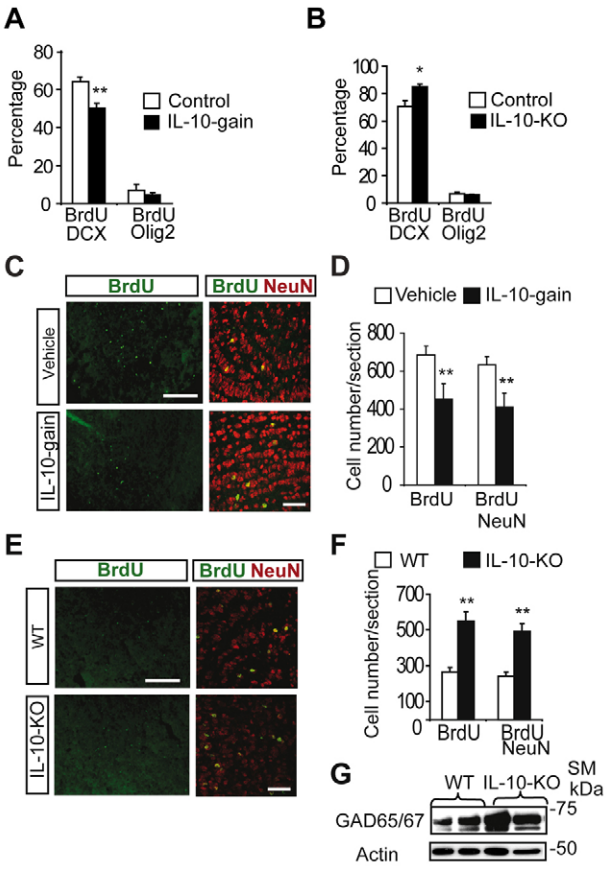

Fig. 7. IL-10 specifically regulates neuronal differentiation in adult SVZ and modulates final OB neurogenesis. (A) Histograms summarize cellular fate determination (expressed as a percentage) on animals injected with BrdU at time 0 and pump implanted over 4 days. Neuronal fate determination ($BrdU^+$, DCX^+) was reduced and glial production ($BrdU^+$, $Olig2^+$) was unaltered by IL-10 ($n=5$). (B) Histogram representing a robust increase in the proportion of newborn determined neurons ($BrdU^+$, DCX^+) in the dorsal SVZ of IL-10-KO animals that received a single dose of BrdU 4 days before sacrifice. Glial determination ($BrdU^+$, $Olig2^+$) was unaltered ($n=6$). (C) The OB showing the presence of $BrdU^+$ and $BrdU^+/NeuN^+$ cells in IL-10 gain-of-function mice. The number of newborn cells ($BrdU^+$) and neurons ($BrdU^+/NeuN^+$) were reduced in the animals where IL-10 activity was induced. (D) Histograms summarizing the quantification of total number of newborn cells and neurons per section in OB of control and IL-10 mice ($n=5$). The number of newborn cells ($BrdU^+$) and neurons ($BrdU^+$, $NeuN^+$) is reduced in the presence of IL-10. (E) OB showing the presence of $BrdU^+$ and $BrdU^+/NeuN^+$ cells in WT and KO mice. (F) Graph represents the total number of newborn cells ($BrdU^+$) and neurons ($BrdU^+$, $NeuN^+$) per OB section. IL-10 deficiency increases the presence of newborn cells and neurons ($n=5$). (G) Protein expression of GAD65/67 on OB samples of WT and IL-10-KO mice. The presence of the GABA-synthesizing enzyme is increased in the absence of IL-10 ($n=4$). Scale bars: 100 μm (A,C, top) and 25 μm (A,C, bottom). Data are means ± s.e.m.; $*P\leq0.05$, $**P\leq0.01$.

revealed that the presence of GAD 65/67, as a marker of GABAergic cells, the extensively main neuronal phenotype of SVZ-derived cells, was increased in samples from IL-10-KO mice (Fig. 7G).

Together, these results indicate that IL-10 activity participates in the control of neurogenesis in the adult SVZ. IL-10 maintains SVZ neural progenitors in an undifferentiated condition, thereby confining neuronal differentiation; consequently, this cytokine regulates the final production of new neurons that will later regenerate the OB.

Discussion

The SVZ niche is a complex system composed of progenitors, the lateral ventricle limited by the ciliated ependymal cells and the vascular system. The niche determines important properties of the stem cell biology including self-renewal, proliferation, differentiation and fate (Suh et al., 2009). Two types of progenitors are present in the SVZ niche: type B and type C cells. Type B cells are exposed to the ventricle and contact with blood vessels. Type C cells do not contact the ventricular space but contact blood vessels (Doetsch et al., 1996; Lois et al., 1994; Merkle et al., 2004). Here we propose a new biological role for IL-10, by which it modulates adult neurogenesis by targeting the $Nestin^+$ progenitors located in the dorsal SVZ.

The adult SVZ is an extensive area where proliferation and neurogenesis occur along the entire rostrocaudal and dorsoventral axes (Mirzadeh et al., 2008). Several studies based on stem cell targeting (Merkle et al., 200743), cell grafting or transcription-factor-based fate mapping show that the NSCs present in various SVZ regions generate distinct types of neurons. In particular, deep granule interneurons and a subpopulation of periglomerular cells arise from the ventral SVZ, whereas superficial granule interneurons, distinct periglomerular cells and glutamatergic cells are derived from the dorsal SVZ (Kelsch et al., 2007; Kohwi et al., 2007; Merkle et al., 2007; Young et al., 2007; Brill et al., 2009). The molecular mechanisms controlling such positional specification are little known. The specific presence of Shh signaling in the ventral SVZ is instructive in cell fate specification and the generation of specific neuronal subtypes (Ihrie et al., 2011). Our data indicate the presence of molecular patterning in the adult SVZ that distinguishes, in a general manner, the dorsal versus ventral region. Progenitors generated along the entire ventral and dorsal regions of the SVZ move from the walls of the LV to reach more anterior dorsal SVZ regions (Kakita and Goldman, 1999; Geraerts et al., 2006; Sawamoto et al., 2006; Nam et al., 2007). IL-10R1 was not expressed in $Nestin^+$ progenitors when these cells were in the ventral SVZ whereas it was expressed in nearly all $Nestin^+$ progenitors located in the dorsal SVZ and ready to enter the RMS to reach their final target, the OB. This open dorsal IL-10R1 expression confers IL-10 the capacity to control final neurogenesis by acting on a wide population of SVZ $Nestin^+$ progenitors, independently of their origin. Our data demonstrate a general action of IL-10 in the regulation of SVZ neuronal differentiation. This is one of the first molecular mechanisms described to be active in the dorsal region of the adult SVZ, which controls neurogenesis. In the future, it would be interesting to address the relevance of IL-10 on interneuron diversity specification and/or the determination of the glutamatergic neuronal phenotype.

The equilibrium between pro- and anti-inflammatory signals in the healthy body is required for the regular physiology of most tissues, including the brain. Here we show that an alteration of IL-10 expression (either gain- or loss-of-function) induces an abnormal ratio of neuronal differentiation in the adult neurogenic niche. As a final consequence, a significant impairment in the number of new neurons regenerating the OB is induced. The interaction of progenitors with the ventricular region and vessels makes these cells susceptible to regulation by local and systemic factors. A decline in neurogenesis and cognitive impairments

observed during aging are associated with changes in blood factors, such as chemokines (Villeda et al., 2011). The CSF and blood of healthy animals contain low concentrations of IL-10, and after CNS inflammation or injury circulating levels of this cytokine increase. Furthermore, neurons and glial cells are also able to produce IL-10 (Lacki et al., 1995; Vila et al., 2003; Yasuda et al., 2008; Bromander et al., 2012). Our data indicate that IL-10 levels are determinants of the normal regulation of adult SVZ neurogenesis (summarized in Fig. 8). IL-10 levels regularly circulate in the body and are upregulated in response to disease, lesion or infection. Therefore, IL-10 could be a sensor of body physiology, continuously providing inputs to the SVZ niche in order to regulate final neurogenesis (summarized in Fig. 8).

Adult neurogenic niches increase proliferation and cell differentiation in response to cerebral aggression and neurodegeneration, but the maintenance of newly generated neurons is compromised (Arvidsson et al., 2002; Baron et al., 2008; Jin et al., 2004; Kokaia et al., 2006). The acute activation of local or systemic innate pro-inflammatory cascades is detrimental for progenitor proliferation. Much research effort has been dedicated to studying the cellular effects of these pro-inflammatory cytokines in an inflammatory context (Ekdahl et al., 2003; Monje et al., 2003). Following these first observations, other pro-inflammatory molecules and their receptors have been associated with the negative regulation of progenitor proliferation (Baron et al., 2008; Gómez-Nicola et al., 2011; Iosif et al., 2006; Koo et al., 2008; Li et al., 2010; Wachs et al., 2006). In addition, some pro-inflammatory signals have been linked to neuronal differentiation (Baron et al., 2008; Li et al., 2010). The molecular and cellular mechanisms that mediate the activity of these cytokines, as well as the relevance of these molecules in SVZ biology, are unclear. Furthermore, little is known about the effects of anti-inflammatory cytokines on SVZ biology in health or in diseased states. In animal models of neurodegeneration, the administration of high doses of IL-10 as an anti-inflammatory agent improves functional parameters and progenitor proliferation (Kiyota et al., 2012; Yang et al., 2009). On the basis of our findings, we propose that increases in systemic IL-10 levels cause a downregulation of SVZ neurogenesis by directly delaying the normal activity of the neurogenic niche (summarized in Fig. 8).

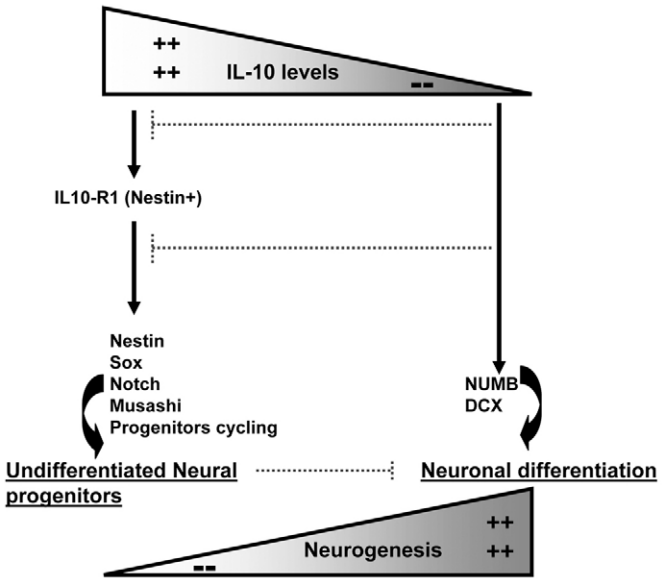

Fig. 8. IL-10 levels modulate adult neurogenesis. The presence of IL-10 leads to the accumulation of undifferentiated neural progenitor markers (Nestin, Sox1, Sox2, Mash1) and members of the Notch pathway (NICD, Musashi) and keeps progenitors cycling (Ki67, pCDC42). As a consequence, neuronal differentiation is reduced. When IL-10 levels are compromised this gene balance is reversed and neuronal gene expression becomes more prevalent, causing an increase in neurogenesis.

Here we report for the first time a novel endogenous action of IL-10 on adult neural progenitors in the healthy brain. IL-10R1 is present in the dorsal SVZ niche, and its expression is restricted to Nestin^{+} progenitors when these cells are located in that area before migrating to the OB. IL-10 directly acts on neural cells from the dorsal SVZ. It promotes a cellular non-differentiating stage and impedes neuronal differentiation among the entire pool progenitors. *In vivo* animal models of IL-10 gain- and loss-of-function showed that alterations in the levels of this cytokine lead to defects in neurogenesis in the healthy adult mouse brain.

Future studies will be crucial to identify the specific intracellular signaling pathways activated by IL-10 in adult brain progenitors and the effects of this cytokine on endogenous neurogenesis in a brain injury context involving the induction of a complex inflammatory process.

Materials and Methods

Recombinant proteins, reagents and animals

IL-10 was purchased from Prepotech (Rocky Hill, CT) and R&D (Minneapolis, MA), and U0126 was from Merck-Millipore (Darmstadt, Germany). Rodents were obtained from Charles River (Lille, France) and IL-10-KO mice (Kuhn et al., 1993) were originally purchased from the Jackson Laboratory. All animals were male and age-matched. Mice for knockout studies were obtained by crossing heterozygote animals. Cerebral volume was measured *in vivo* by MRI in WT and IL-10-KO mice. Mice were scanned in a 7.0 T BioSpec 70/30 horizontal animal scanner (Bruker BioSpin, Ettlingen, Germany). The analysis of T2 maps using AMIRA software or ImageJ showed no differences in forebrain volume between the two genotypes. Animals were kept and treated in accordance with the European Community Council Directive on animal welfare. Every effort was made to minimize animal suffering.

Primary cultures

We studied IL-10 and its receptors in the postnatal and adult SVZ niche of both rat and mouse brains. Cell cultures were performed from postnatal brains of rats and mice (P7–P9) because cell viability, amount of material and adherence was better compared with adult cultures, and this reduced the number of animals needed per experiment. Fresh rat and mice coronal sections were obtained from the anterior forebrain using a McIlwain tissue chopper (300–500 µm). The SVZ was gently microdissected from each coronal section with the aid of sharpened metallic needles. Since dissociated mice brain cells did not attach properly in differentiating conditions, cultures were prepared from rat brain.

Neurospheres

Dorsal SVZ was digested by trypsin and cultured in the presence of 10 ng/ml bFGF and 20 ng/ml of EGF in DMEM/F12 medium plus supplements (Life Technologies). Self-renewal studies were performed as described previously in different passages (Ferron et al., 2007). Differences between neurosphere cultures prepared from postnatal and adult brains have been described (Gritti et al., 2009). Differentiation studies were performed by mechanical dissociation of neurospheres from passage 2 in DMEM/F12 medium with B27 in the presence or absence of IL-10 (50 ng/ml) for 7 days.

Dissociated cultures

Freshly isolated SVZ was mildly trypsinized and plated in poly-L-lysine-coated plates at medium density (40,000 cells/well on 48-well plates) and cultured in DMEM/F12 supplemented with B27 (Life Technologies, Paisley, UK) in the presence or absence of IL-10 (50 ng/ml) for several days. For viability studies, living cultures were stained with 10 µg propidium iodide (PI) to specifically label dead cells and all nuclei were stained with Hoechst 33342. A concentration-response curve was performed in order to determine the working concentration. Cell death was represented as percentage of the total number of cells. Proliferative

studies were analyzed after a 4 hour pulse of bromo-deoxy-uridine (BrdU, 10 μM; Sigma-Aldrich, St Louis, MO) for each time studied. Pulse–chase experiments were performed 12 hours after platting dissociated primary cells; a pulse of 90 minutes of BrdU was applied to the cells and cells were chased at different time points (between 90 minutes and 12 hours) in order to study the S–G2–M transition. Dissociated cultures were fixed at each time point for 10 minutes in 4% paraformaldehyde (PFA). Cells were permeabilized with 0.1% Triton X-100 and stained as below. Nuclei were routinely counterstained with Hoechst 33342.

Explants

Isolated postnatal dorsal SVZ was cut in explants and embedded in Matrigel (BD-Bioscience), IL-10 was added at (50 ng/ml). Culture conditions and cell migration were described previously (Pozas and Ibáñez, 2005).

Biochemistry

Western blotting was carried out after primary cultures and tissue samples were lysed and sonicated in RIPA buffer with proteases and phosphatase inhibitors. Protein was quantified by BCA (Pierce, Waltham, MA) and run in SDS-PAGE gels and transferred to PVDF membranes (Merck-Millipore). 5 μg total protein from culture lysates and 20–40 μg from tissue samples were loaded on polyacrylamide gels. Membranes were then incubated with $pCDC2_{Tyr15}$ (Cell Signaling Technology; 1:1000), DCX (Cell Signaling Technology; 1:1000; Santa Cruz Biotechnology, Santa Cruz, CA; 1:500), Sox1 (Merck-Millipore; 1:500), Sox2 (Merck-Millipore; 1:500), Nestin (1:500; either from Hybridoma Bank, Merck-Millipore or BD Bioscience San Jose, CA), Musashi (Millipore; 1:500), Mash1 (BD Bioscience; 1:500), total STAT-1 (BD Transduction; 1:1000), total STAT-3 (BD Bioscience; 1:1000), total CDC2 (Cell Signaling; 1:1000), Notch-ICD (Abcam, Cambridge, UK; 1:500), Numb (Abcam; 1:500); GFAP (DAKO, Glostrup, Denmark; 1:50,000), GAD 65/67 (Assay Designs, Lausen, Switzerland; 1:1000), Spectrin (Millipore; 1:1000) and Tubulin (Sigma; 1:50,000) or Actin (Sigma; 1:50,000) as loading controls. Blots were then processed by secondary antibodies conjugated to horseradish peroxidase and developed using luminol on X-ray films. Films were scanned and analyzed by Quantity One (Bio-Rad, Hercules, CA).

RT-PCR

Total RNA from different cell culture samples and brain from postnatal ages of both mice and rats was isolated with SNAP columns (Life Technologies) or Trizol. Single-stranded cDNA was synthesized using AMV First-Strand cDNA Synthesis KIT (Life Technologies) and subjected to PCR. GenBank cDNA sequences were used to design gene specific primers in Primer3 Output and their specificity was determined by BLAST searching. Primer sequences were: rat IL-10 (ID, NM_12854) forward 5′-CCTGCTCTTACTGGCTGGAG-3′ and reverse 5′-TGTCCAGCTGGTCCTTCTTT-3′; mouse IL-10 (ID, NM_010548) forward 5′-AGTGAGAAGCTGAAGACCCTCAGG-3′ and reverse 5′-TTCATGGCCTTGT-AGACACCTTGGT-3′, rat IL-10R1 (ID, NM_057193) forward 5′-TGAAAC-TCGCTTCACAGTGG-3′ and reverse 5′-TAAATACGGTGGTGCGTGAA-3′; mouse IL-10R1 (ID, L12120) forward 5′-AAAGGCTCAGGCATTGTCCT-3′ and reverse 5′-TCACGCTATCCACTGTCAGA-3′.

Immunofluorescence

Primary antibodies (as described above) were used at the following dilutions: TUBB3 (1:1000), DCX (1:1000), Nestin (1:200), Ki67 (Leica Microsystems, Wetzlar, Germany; 1:1000), pCDC2 (1:300); PH3 (1:500; Cell Signaling Technology), IL-10R1 (1:150; from Millipore or Santa Cruz Biotechnology), BrdU (AbCam; 1:400), NG2 (Millipore; 1:400), GFAP (DAKO; 1:2000), NeuN (Millipore; 1:1000), Gad67 (Millipore; 1:300) and Spectrin (Millipore; 1:1000). Following the first immunoreaction, samples were incubated with secondary antibodies conjugated with Alexa Fluor dyes (Molecular Probes; 1:1000). In some cases, staining was amplified by secondary biotinylated antibodies (Vector; 1:200) followed by Alexa-Streptavidin (Molecular Probes; 1:500). Staining on cell cultures was visualized with a Leica CTR400-DMI400B inverted microscope. Photographs were taken with a DFC300FX camera from Leica. Quantification was carried out using Leica Application Suite (LAS-Leica) or ImageJ (NIH) software. The number of positive cells for each experimental assay was expressed as percentage of the total number, and/or referred as percentage of the control.

In vivo IL-10 administration

Intracerebroventricular IL-10 infusion in mouse brain

The administration of IL-10 (50 ng/ml) and/or U0126 (25 μM) in the lateral ventricle was carried out by continuous infusion with Alzet osmotic minipumps (model 1007D) and Alzet Brain Infusion Kit 3 (DURECT Corporation, Cupertino, CA). The animal was placed in a stereotaxic frame using a mice adaptor (Stoelting, Wood Dale, IL) and the delivery of saline or IL-10 to the lateral ventricle of the right hemisphere was achieved by inserting the cannula 1.7 mm deep from the brain surface at −0.1 mm posterior, and 0.6 lateral coordinates from Bregma. The cannula was connected to the osmotic minipump placed in a subcutaneous pocket between the scapulae. Infusion of vehicle, IL-10 (50 ng/ml) was carried out at a low flow rate of 0.5 μl/hour and it was prolonged during 4 (4-day-treated animals) and/or 7 days (7-day-treated animals) depending on the experimental group. Contralateral hemisphere (left) was always considered for histological analysis and some ipsilateral hemispheres were used for biochemical studies.

In vivo BrdU injections

Intraperitoneal (IP) BrdU injections were administered in three independent experimental groups. In the first group, the animals received BrdU (50 mg/kg) daily for 7 days until the day of sacrifice. In the second group, animals received a single dose of BrdU at day 0 and were killed at day 4. The last group of animals received BrdU on the two first days (0 and 1) and were perfused at day 19. These BrdU injections were performed in the IL-10 gain-of-function animal model and in IL-10-KO mice.

Histology

Tissue fixation

Postnatal and adult animals (8 weeks) were always perfused with saline followed by 4% paraformaldehyde and cryoprotected in 30% sucrose. The forebrain was snap-frozen in dry-ice and coronal sections (16 μm) were obtained and were collected in eight consecutive slice series. Slices were frozen and were air-dried at room temperature before use for histological analyses. In all animals, the left (contralateral) hemisphere was analyzed on histological sections to avoid any mechanical damage that might be caused by inserting the delivery cannula in the right ventricle.

Total number and cell death evaluation

Routinely, the evaluation of total number of cells present in the dorsal SVZ was carried out after TO-PRO staining (Invitrogen). Cell death was evaluated by morphological observation and cleaved Caspase 3 immunostaining (Cell Signaling; 1:150). Cell death was also evaluated by the pattern of cleaved Spectrin by elecrophoresis and western blotting (see above).

Immunofluorescence on tissue sections

The primary antibodies used for immunofluorescence were as described above. Brain sections were scanned and evaluated under a Leica DM5500Q confocal microscope. At least four consecutive sections from the same slice were evaluated for each staining and the number of positive cells for each section was counted after a *Z* projection by ImageJ or LAS (Leica application suite) software. For the SVZ analysis, images were taken between +1.10 mm and +0.38 mm from Bregma. For OB studies, we analyzed a number of consecutives series starting around +3.56 from Bregma and going rostrally. The total number of cells per section or the percentages of a particular cell population were represented on the histograms.

Statistical analysis

Analyses of significant differences between group means were performed using the two-tailed Student's *t*-tests. In each case, *n* indicates the number of independent cultures or mice used. Statistical significance was considered where $P<0.05$.

Acknowledgements

We are grateful to Dr Fernando Aguado for helpful discussions, and Toffa Evans and Amanda Billington for editorial assistance. We are indebted to the Cytomics and Image Units of the Institut d'Investigacions Biomèdiques August Pi i Sunyer (IDIBAPS) for technical help. Some Nestin antibodies were obtained from the Developmental Studies Hybridoma Bank at the University of Iowa.

Funding

This work was supported by Carlos III Health Institute, Spain [grant number PI070917 to E.P.]; Marató TV3 [grant number 279/U2011 to E.P.]; Start-up grants from the Ministerio de Ciencia e Innovación (MICINN) and IDIBAPS [to E.P.]; Plan Nacional from MICINN [grant number SAF2011-30492 to A.M.P.]; E.P. is a researcher of the Ramón y Cajal program (MICINN).

Author contributions

F.P.A. and U.P. performed the research; A.M.P helped in the design and financial support at the start of the research, and approved the final version of the manuscript; E.P. performed, designed and supervised research, and wrote the manuscript.

Supplementary material available online at
http://jcs.biologists.org/lookup/suppl/doi:10.1242/jcs.127803/-/DC1

References

Abrieu, A., Fisher, D., Simon, M. N., Dorée, M. and Picard, A. (1997). MAPK inactivation is required for the G2 to M-phase transition of the first mitotic cell cycle. *EMBO J.* **16**, 6407-6413.

Aguirre, A., Rubio, M. E. and Gallo, V. (2010). Notch and EGFR pathway interaction regulates neural stem cell number and self-renewal. *Nature* **467**, 323-327.

Andreu-Agulló, C., Morante-Redolat, J. M., Delgado, A. C. and Fariñas, I. (2009). Vascular niche factor PEDF modulates Notch-dependent stemness in the adult subependymal zone. *Nat. Neurosci.* **12**, 1514-1523.

Androutsellis-Theotokis, A., Leker, R. R., Soldner, F., Hoeppner, D. J., Ravin, R., Poser, S. W., Rueger, M. A., Bae, S. K., Kittappa, R. and McKay, R. D. (2006). Notch signalling regulates stem cell numbers in vitro and in vivo. *Nature* **442**, 823-826.

Arvidsson, A., Collin, T., Kirik, D., Kokaia, Z. and Lindvall, O. (2002). Neuronal replacement from endogenous precursors in the adult brain after stroke. *Nat. Med.* **8**, 963-970.

Baron, R., Nemirovsky, A., Harpaz, I., Cohen, H., Owens, T. and Monsonego, A. (2008). IFN-gamma enhances neurogenesis in wild-type mice and in a mouse model of Alzheimer's disease. *FASEB J.* **22**, 2843-2852.

Brill, M. S., Ninkovic, J., Winpenny, E., Hodge, R. D., Ozen, I., Yang, R., Lepier, A., Gascón, S., Erdelyi, F., Szabo, G. et al. (2009). Adult generation of glutamatergic olfactory bulb interneurons. *Nat. Neurosci.* **12**, 1524-1533.

Doetsch, F. and Alvarez-Buylla, A. (1996). Network of tangential pathways for neuronal migration in adult mammalian brain. *Proc. Natl. Acad. Sci. USA* **93**, 14895-14900.

Doetsch, F., García-Verdugo, J. M. and Alvarez-Buylla, A. (1997). Cellular composition and three-dimensional organization of the subventricular germinal zone in the adult mammalian brain. *J. Neurosci.* **17**, 5046-5061.

Doetsch, F., García-Verdugo, J. M. and Alvarez-Buylla, A. (1999). Regeneration of a germinal layer in the adult mammalian brain. *Proc. Natl. Acad. Sci. USA* **96**, 11619-11624.

Ekdahl, C. T., Claasen, J. H., Bonde, S., Kokaia, Z. and Lindvall, O. (2003). Inflammation is detrimental for neurogenesis in adult brain. *Proc. Natl. Acad. Sci. USA* **100**, 13632-13637.

Fernando, R. N., Eleuteri, B., Abdelhady, S., Nussenzweig, A., Andäng, M. and Ernfors, P. (2011). Cell cycle restriction by histone H2AX limits proliferation of adult neural stem cells. *Proc. Natl. Acad. Sci. USA* **108**, 5837-5842.

Ferron, S. R., Andreu-Agullo, C., Mira, H., Sanchez, P., Marques-Torrejon, M. A. and Farinas, I. (2007). A combined ex/in vivo assay to detect effects of exogenously added factors in neural stem cells. *Nat. Protoc.* **2**, 849-859.

Geraerts, M., Eggermont, K., Hernandez-Acosta, P., Garcia-Verdugo, J. M., Baekelandt, V. and Debyser, Z. (2006). Lentiviral vectors mediate efficient and stable gene transfer in adult neural stem cells in vivo. *Hum. Gene Ther.* **17**, 635-650.

Gómez-Nicola, D., Valle-Argos, B., Pallas-Bazarra, N. and Nieto-Sampedro, M. (2011). Interleukin-15 regulates proliferation and self-renewal of adult neural stem cells. *Mol. Biol. Cell* **22**, 1960-1970.

Gonzalez, P., Burgaya, F., Acarin, L., Peluffo, H., Castellano, B. and Gonzalez, B. (2009). Interleukin-10 and interleukin-10 receptor-I are upregulated in glial cells after an excitotoxic injury to the postnatal rat brain. *J. Neuropathol. Exp. Neurol.* **68**, 391-403.

Gonzalez-Perez, O., Romero-Rodriguez, R., Soriano-Navarro, M., Garcia-Verdugo, J. M. and Alvarez-Buylla, A. (2009). Epidermal growth factor induces the progeny of subventricular zone type B cells to migrate and differentiate into oligodendrocytes. *Stem Cells* **27**, 2032-2043.

Gritti, A., Dal Molin, M., Foroni, C. and Bonfanti, L. (2009). Effects of developmental age, brain region, and time in culture on long-term proliferation and multipotency of neural stem cell populations. *J. Comp. Neurol.* **517**, 333-349.

Guillemot, F. (2007). Spatial and temporal specification of neural fates by transcription factor codes. *Development* **134**, 3771-3780.

Ihrie, R. A., Shah, J. K., Harwell, C. C., Levine, J. H., Guinto, C. D., Lezameta, M., Kriegstein, A. R. and Alvarez-Buylla, A. (2011). Persistent sonic hedgehog signaling in adult brain determines neural stem cell positional identity. *Neuron* **71**, 250-262.

Imai, T., Tokunaga, A., Yoshida, T., Hashimoto, M., Mikoshiba, K., Weinmaster, G., Nakafuku, M. and Okano, H. (2001). The neural RNA-binding protein Musashi1 translationally regulates mammalian numb gene expression by interacting with its mRNA. *Mol. Cell. Biol.* **21**, 3888-3900.

Iosif, R. E., Ekdahl, C. T., Ahlenius, H., Pronk, C. J., Bonde, S., Kokaia, Z., Jacobsen, S. E. and Lindvall, O. (2006). Tumor necrosis factor receptor 1 is a negative regulator of progenitor proliferation in adult hippocampal neurogenesis. *J. Neurosci.* **26**, 9703-9712.

Jin, K., Galvan, V., Xie, L., Mao, X. O., Gorostiza, O. F., Bredesen, D. E. and Greenberg, D. A. (2004). Enhanced neurogenesis in Alzheimer's disease transgenic (PDGF-APPSw,Ind) mice. *Proc. Natl. Acad. Sci. USA* **101**, 13363-13367.

Kakita, A. and Goldman, J. E. (1999). Patterns and dynamics of SVZ cell migration in the postnatal forebrain: monitoring living progenitors in slice preparations. *Neuron* **23**, 461-472.

Kelsch, W., Mosley, C. P., Lin, C. W. and Lois, C. (2007). Distinct mammalian precursors are committed to generate neurons with defined dendritic projection patterns. *PLoS Biol.* **5**, e300.

Khodosevich, K., Watanabe, Y. and Monyer, H. (2011). EphA4 preserves postnatal and adult neural stem cells in an undifferentiated state in vivo. *J. Cell Sci.* **124**, 1268-1279.

Kiyota, T., Ingraham, K. L., Swan, R. J., Jacobsen, M. T., Andrews, S. J. and Ikezu, T. (2012). AAV serotype 2/1-mediated gene delivery of anti-inflammatory interleukin-10 enhances neurogenesis and cognitive function in APP+PS1 mice. *Gene Ther.* **19**, 724-733.

Kohwi, M., Petryniak, M. A., Long, J. E., Ekker, M., Obata, K., Yanagawa, Y., Rubenstein, J. L. and Alvarez-Buylla, A. (2007). A subpopulation of olfactory bulb GABAergic interneurons is derived from Emx1- and Dlx5/6-expressing progenitors. *J. Neurosci.* **27**, 6878-6891.

Kokaia, Z., Thored, P., Arvidsson, A. and Lindvall, O. (2006). Regulation of stroke-induced neurogenesis in adult brain—recent scientific progress. *Cereb. Cortex* **16 Suppl. 1**, i162-i167.

Koo, J. W. and Duman, R. S. (2008). IL-1beta is an essential mediator of the antineurogenic and anhedonic effects of stress. *Proc. Natl. Acad. Sci. USA* **105**, 751-756.

Kühn, R., Löhler, J., Rennick, D., Rajewsky, K. and Müller, W. (1993). Interleukin-10-deficient mice develop chronic enterocolitis. *Cell* **75**, 263-274.

Kuo, C. T., Mirzadeh, Z., Soriano-Navarro, M., Rasin, M., Wang, D., Shen, J., Sestan, N., Garcia-Verdugo, J., Alvarez-Buylla, A., Jan, L. Y. et al. (2006). Postnatal deletion of Numb/Numblike reveals repair and remodeling capacity in the subventricular neurogenic niche. *Cell* **127**, 1253-1264.

Kyritsis, N., Kizil, C., Zocher, S., Kroehne, V., Kaslin, J., Freudenreich, D., Iltzsche, A. and Brand, M. (2012). Acute inflammation initiates the regenerative response in the adult zebrafish brain. *Science* **338**, 1353-1356.

Lacki, J. K., Klama, K., Mackiewicz, S. H., Mackiewicz, U. and Müller, W. (1995). Circulating interleukin 10 and interleukin-6 serum levels in rheumatoid arthritis patients treated with methotrexate or gold salts: preliminary report. *Inflamm. Res.* **44**, 24-26.

Levy, D. E. and Darnell, J. E., Jr (2002). Stats: transcriptional control and biological impact. *Nat. Rev. Mol. Cell Biol.* **3**, 651-662.

Li, H. S., Wang, D., Shen, Q., Schonemann, M. D., Gorski, J. A., Jones, K. R., Temple, S., Jan, L. Y. and Jan, Y. N. (2003). Inactivation of Numb and Numblike in embryonic dorsal forebrain impairs neurogenesis and disrupts cortical morphogenesis. *Neuron* **40**, 1105-1118.

Li, L., Walker, T. L., Zhang, Y., Mackay, E. W. and Bartlett, P. F. (2010). Endogenous interferon gamma directly regulates neural precursors in the non-inflammatory brain. *J. Neurosci.* **30**, 9038-9050.

Lim, D. A., Huang, Y. C., Swigut, T., Mirick, A. L., Garcia-Verdugo, J. M., Wysocka, J., Ernst, P. and Alvarez-Buylla, A. (2009). Chromatin remodelling factor Mll1 is essential for neurogenesis from postnatal neural stem cells. *Nature* **458**, 529-533.

Lois, C. and Alvarez-Buylla, A. (1994). Long-distance neuronal migration in the adult mammalian brain. *Science* **264**, 1145-1148.

Marqués-Torrejón, M. A., Porlan, E., Banito, A., Gómez-Ibarlucea, E., Lopez-Contreras, A. J., Fernández-Capetillo, O., Vidal, A., Gil, J., Torres, J. and Fariñas, I. (2013). Cyclin-dependent kinase inhibitor p21 controls adult neural stem cell expansion by regulating Sox2 gene expression. *Cell Stem Cell* **12**, 88-100.

Marshall, C. A., Novitch, B. G. and Goldman, J. E. (2005). Olig2 directs astrocyte and oligodendrocyte formation in postnatal subventricular zone cells. *J. Neurosci.* **25**, 7289-7298.

Menn, B., Garcia-Verdugo, J. M., Yaschine, C., Gonzalez-Perez, O., Rowitch, D. and Alvarez-Buylla, A. (2006). Origin of oligodendrocytes in the subventricular zone of the adult brain. *J. Neurosci.* **26**, 7907-7918.

Merkle, F. T., Tramontin, A. D., García-Verdugo, J. M. and Alvarez-Buylla, A. (2004). Radial glia give rise to adult neural stem cells in the subventricular zone. *Proc. Natl. Acad. Sci. USA* **101**, 17528-17532.

Merkle, F. T., Mirzadeh, Z. and Alvarez-Buylla, A. (2007). Mosaic organization of neural stem cells in the adult brain. *Science* **317**, 381-384.

Mirzadeh, Z., Merkle, F. T., Soriano-Navarro, M., Garcia-Verdugo, J. M. and Alvarez-Buylla, A. (2008). Neural stem cells confer unique pinwheel architecture to the ventricular surface in neurogenic regions of the adult brain. *Cell Stem Cell* **3**, 265-278.

Mobley, A. K., Tchaicha, J. H., Shin, J., Hossain, M. G. and McCarty, J. H. (2009). Beta8 integrin regulates neurogenesis and neurovascular homeostasis in the adult brain. *J. Cell Sci.* **122**, 1842-1851.

Monje, M. L., Toda, H. and Palmer, T. D. (2003). Inflammatory blockade restores adult hippocampal neurogenesis. *Science* **302**, 1760-1765.

Nam, S. C., Kim, Y., Dryanovski, D., Walker, A., Goings, G., Woolfrey, K., Kang, S. S., Chu, C., Chenn, A., Erdelyi, F. et al. (2007). Dynamic features of postnatal subventricular zone cell motility: a two-photon time-lapse study. *J. Comp. Neurol.* **505**, 190-208.

Nishimoto, Y. and Okano, H. (2010). New insight into cancer therapeutics: induction of differentiation by regulating the Musashi/Numb/Notch pathway. *Cell Res.* **20**, 1083-1085.

Ouyang, W., Rutz, S., Crellin, N. K., Valdez, P. A. and Hymowitz, S. G. (2011). Regulation and functions of the IL-10 family of cytokines in inflammation and disease. *Annu. Rev. Immunol.* **29**, 71-109.

Parras, C. M., Galli, R., Britz, O., Soares, S., Galichet, C., Battiste, J., Johnson, J. E., Nakafuku, M., Vescovi, A. and Guillemot, F. (2004). Mash1 specifies neurons and oligodendrocytes in the postnatal brain. *EMBO J.* **23**, 4495-4505.

Pastrana, E., Silva-Vargas, V. and Doetsch, F. (2011). Eyes wide open: a critical review of sphere-formation as an assay for stem cells. *Cell Stem Cell* **8**, 486-498.

Pestka, S., Krause, C. D., Sarkar, D., Walter, M. R., Shi, Y. and Fisher, P. B. (2004). Interleukin-10 and related cytokines and receptors. *Annu. Rev. Immunol.* **22**, 929-979.

Petersen, P. H., Zou, K., Krauss, S. and Zhong, W. (2004). Continuing role for mouse Numb and Numbl in maintaining progenitor cells during cortical neurogenesis. *Nat. Neurosci.* **7**, 803-811.

Pozas, E. and Ibáñez, C. F. (2005). GDNF and GFRalpha1 promote differentiation and tangential migration of cortical GABAergic neurons. *Neuron* **45**, 701-713.

Rabaneda, L. G., Carrasco, M., López-Toledano, M. A., Murillo-Carretero, M., Ruiz, F. A., Estrada, C. and Castro, C. (2008). Homocysteine inhibits proliferation of neuronal precursors in the mouse adult brain by impairing the basic fibroblast growth factor signaling cascade and reducing extracellular regulated kinase 1/2-dependent cyclin E expression. *FASEB J.* **22**, 3823-3835.

Ramírez-Castillejo, C., Sánchez-Sánchez, F., Andreu-Agulló, C., Ferrón, S. R., Aroca-Aguilar, J. D., Sánchez, P., Mira, H., Escribano, J. and Fariñas, I. (2006). Pigment epithelium-derived factor is a niche signal for neural stem cell renewal. *Nat. Neurosci.* **9**, 331-339.

Romero-Grimaldi, C., Murillo-Carretero, M., López-Toledano, M. A., Carrasco, M., Castro, C. and Estrada, C. (2011). ADAM-17/tumor necrosis factor-α-converting enzyme inhibits neurogenesis and promotes gliogenesis from neural stem cells. *Stem Cells* **29**, 1628-1639.

Saraiva, M. and O'Garra, A. (2010). The regulation of IL-10 production by immune cells. *Nat. Rev. Immunol.* **10**, 170-181.

Sawamoto, K., Wichterle, H., Gonzalez-Perez, O., Cholfin, J. A., Yamada, M., Spassky, N., Murcia, N. S., Garcia-Verdugo, J. M., Marin, O., Rubenstein, J. L. et al. (2006). New neurons follow the flow of cerebrospinal fluid in the adult brain. *Science* **311**, 629-632.

Suh, H., Deng, W. and Gage, F. H. (2009). Signaling in adult neurogenesis. *Annu. Rev. Cell Dev. Biol.* **25**, 253-275.

Teixeira, C. M., Kron, M. M., Masachs, N., Zhang, H., Lagace, D. C., Martinez, A., Reillo, I., Duan, X., Bosch, C., Pujadas, L. et al. (2012). Cell-autonomous inactivation of the reelin pathway impairs adult neurogenesis in the hippocampus. *J. Neurosci.* **32**, 12051-12065.

Vila, N., Castillo, J., Dávalos, A., Esteve, A., Planas, A. M. and Chamorro, A. (2003). Levels of anti-inflammatory cytokines and neurological worsening in acute ischemic stroke. *Stroke* **34**, 671-675.

Villeda, S. A., Luo, J., Mosher, K. I., Zou, B., Britschgi, M., Bieri, G., Stan, T. M., Fainberg, N., Ding, Z., Eggel, A. et al. (2011). The ageing systemic milieu negatively regulates neurogenesis and cognitive function. *Nature* **477**, 90-94.

Wachs, F. P., Winner, B., Couillard-Despres, S., Schiller, T., Aigner, R., Winkler, J., Bogdahn, U. and Aigner, L. (2006). Transforming growth factor-beta1 is a negative modulator of adult neurogenesis. *J. Neuropathol. Exp. Neurol.* **65**, 358-370.

Yang, J., Jiang, Z., Fitzgerald, D. C., Ma, C., Yu, S., Li, H., Zhao, Z., Li, Y., Ciric, B., Curtis, M. et al. (2009). Adult neural stem cells expressing IL-10 confer potent immunomodulation and remyelination in experimental autoimmune encephalitis. *J. Clin. Invest.* **119**, 3678-3691.

Young, K. M., Fogarty, M., Kessaris, N. and Richardson, W. D. (2007). Subventricular zone stem cells are heterogeneous with respect to their embryonic origins and neurogenic fates in the adult olfactory bulb. *J. Neurosci.* **27**, 8286-8296.